

Review

Boronization and Carburization of Superplastic Stainless Steel and Titanium-Based Alloys

Masafumi Matsushita

Department of Mechanical Engineering, Ehime University, 3-Bunkyocho, Matsuyama 790-8577, Japan; E-Mail: matsushita@eng.ehime-u.ac.jp; Tel.: +81-89-927-9902; Fax: +81-89-927-9902

Received: 28 June 2011 / Accepted: 12 July 2011 / Published: 18 July 2011

Abstract: Boronization and carburization of fine-grain superplastic stainless steel is reviewed, and new experimental results for fine grain $Ti_{88.5}Al_{4.5}V_3Fe_2Mo_2$ are reported. In superplastic duplex stainless steel, the diffusion of carbon and boron is faster than in non-superplastic duplex stainless steel. Further, diffusion is activated by uniaxial compressive stress. Moreover, non-superplastic duplex stainless steel shows typical grain boundary diffusion; however, inner grain diffusion is confirmed in superplastic stainless steel. The presence of Fe and Cr carbides or borides is confirmed by X-ray diffraction, which indicates that the diffused carbon and boron react with the Fe and Cr in superplastic stainless steel. The Vickers hardness of the carburized and boronized layers is similar to that achieved with other surface treatments such as electro-deposition. Diffusion of boron into the superplastic $Ti_{88.5}Al_{4.5}V_3Fe_2Mo_2$ alloy was investigated. The hardness of the surface exposed to boron powder can be increased by annealing above the superplastic temperature. However, the Vickers hardness is lower than that of Ti boride.

Keywords: diffusion; superplasticity; carburization; boronization; duplex stainless steel

1. Introduction

The discussion of superplasticity has been performed in many scientific fields, not only materials science and engineering, but also even in the field of earth science [1-7]. In this review, we have demonstrated the diffusions of carbon and boron into two kinds of fine grain type superplastic materials: one is superplastic duplex stainless steel (SPDSS) and another is titanium based duplex alloy $Ti_{88.5}Al_{4.5}V_3Fe_2Mo_2$ (SP-700).

These alloys are common industrial superplastic materials. Diffusion in the superplastic state is an important research field because diffusion is very important to consider superplastic forming-diffusion

bonding (SPF-DB), further it has prospects for applying surface hardening treatments, such as carburization and boronization. At first, the diffusion of carbon on the SPF-DB interface between high carbon steel and SPDSS is mentioned, and then carburization and boronization processes using solid state diffusion of SPDSS are reviewed. Finally, boronization of SP-700 has been demonstrated.

2. The Diffusion of Carbon at Interface of High Carbon Steel and SPDSS

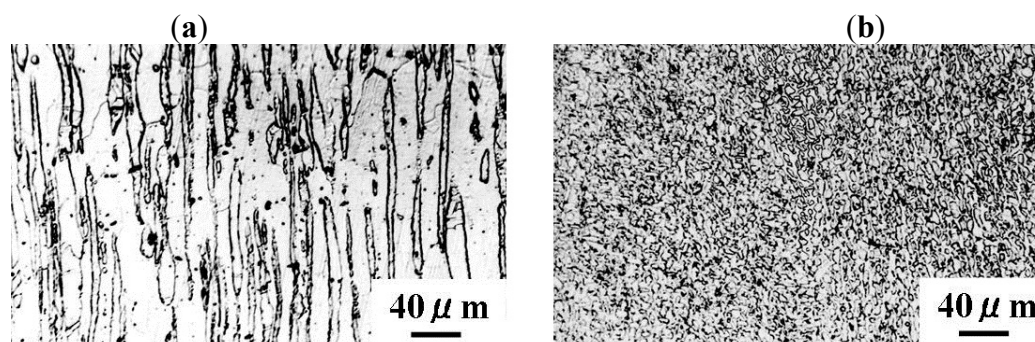
SPF-DB is one of the most important applications of superplasticity. Diffusion taking place on interface is important to consider the strength of SPF-DB. An example, in which diffusion affects the fracture strength of bonded materials by SPF-DB, is mentioned in this section [8,9].

SPDSS is one of the fine grain type superplastic materials. Chemical composition of SPDSS is the same as non-superplastic duplex stainless (DSS) as shown in Table 1. In order to convert DSS to the fine grain type superplastic material, namely SPDSS, the following procedure is needed. First, to obtain a single phase, the DSS is annealed for one hour at 1573 K and then quenched in water. Subsequently, the material is cold rolled. Afterwards, the material is annealed at 1273 K to precipitate the face centered cubic structure (FCC) phase. As a result of the aforementioned treatments, very fine-grain DSS, namely SPDSS as shown in Figure 1, are obtained. The SPDSS shows a superplastic elongation of over 100 % above 1223 K at a strain rate of $1 \times 10^{-4} \text{ s}^{-1}$.

Table 1. Chemical composition of duplex stainless steel (bal. Fe).

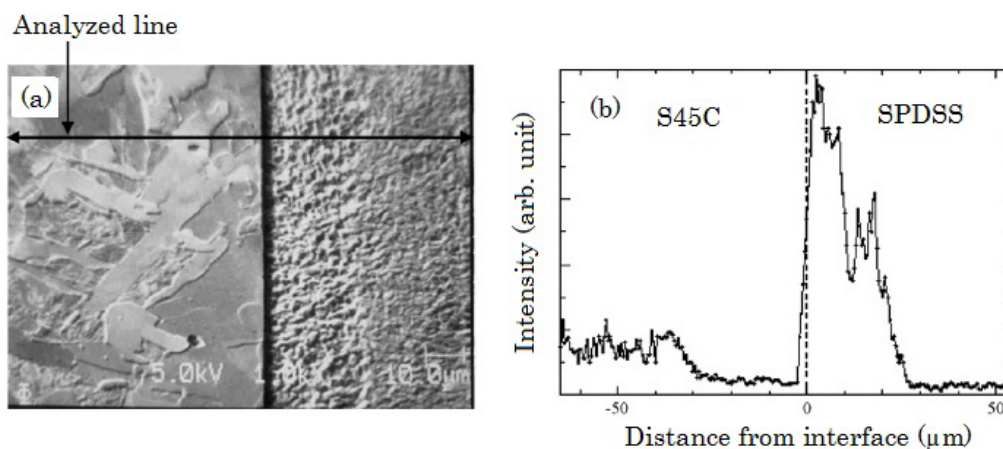
	C	Si	Mn	P	S	Ni	Cr	Mo	N
DSS	0.02	0.36	0.08	0.027	0.007	5.43	23.8	1.23	—

Figure 1. Microscopy image of the texture of (a) non-superplastic DSS and (b) SPDSS.



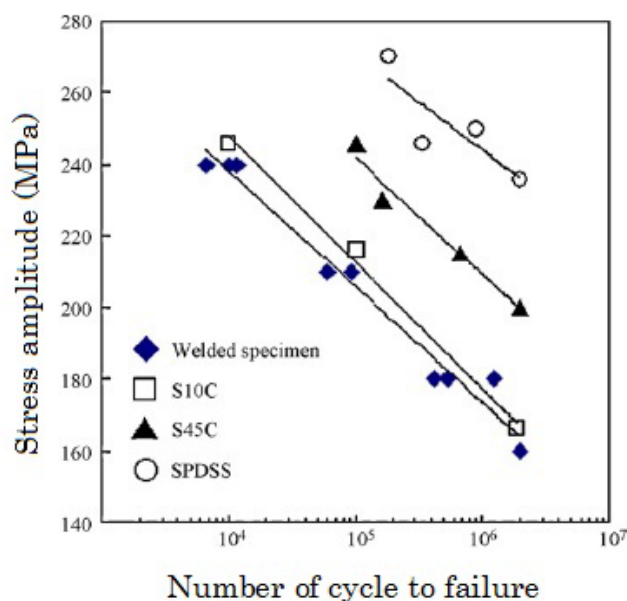
A cross-sectional image of an interface between high carbon steel of carbon content 0.45 wt% (S45C) and SPDSS bonded by the SPF-DB is given in Figure 2a. Bonding condition of this specimen is a compressive stress of 3 MPa at 1373 K for 220 s. A line analysis of the carbon content for cross section of interface bonding obtained by Auger electron spectroscopy (AES) is given in Figure 2b. The carbon content of S45C decreases near the interface. The carbon content in S45C at 10 μm from the interface is approximately 1/4 of the content at a distance of 40 μm from the interface. Conversely, the carbon content in the SPDSS increases near the interface. This result clearly indicates that the carbon in S45C migrates to the SPDSS side of the interface.

Figure 2. Cross-sectional view of the interface between S45C and SPDSS bonded by the SPF-DB method: (a) shows scanning electron micrograph; and (b) line analysis by Auger electron spectroscopy for carbon [8].



The number of cycles to failure (N_f) at various stress amplitudes (σ) of the aforementioned specimen are shown in Figure 3. It can be seen that the N_f - σ line of the S45C-SPDSS bonding specimen is lower than that of S45C and similar to that of carbon steel of carbon content 0.1 wt% (S10C). According to the line analysis by AES, the carbon content of S45C near the interface is 1/4 of the original carbon content of S45C; namely, the carbon content of S45C near the interface is similar to S10C. The N_f - σ line of the S45C-SPDSS bonding specimen can be interpreted by the effect of decarburizing of S45C at the interface.

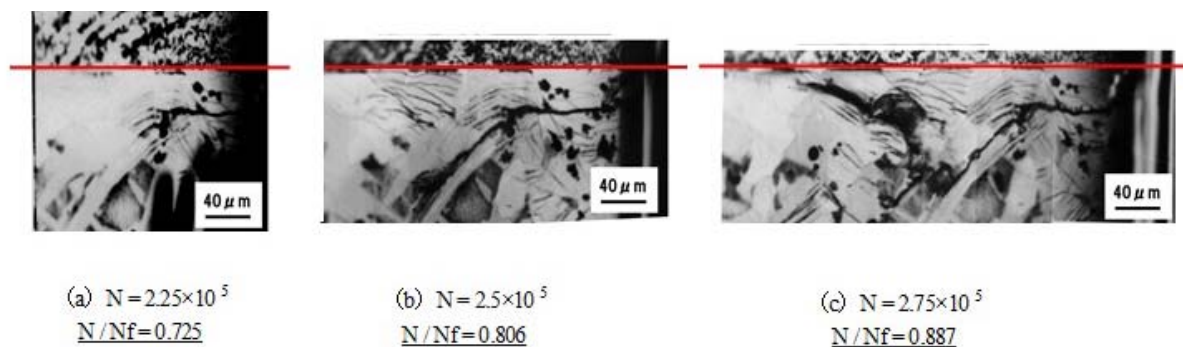
Figure 3. The numbers of cycles to failure at various stress amplitudes for the S45C-SPDSS specimen bonded by SPF-DB, S45C, SPDSS and S10C [8].



Moreover, in order to investigate cracking, micrographs of the interface area were obtained, as shown in Figure 4. The number of cycles is normalized by the fracture number. It can be seen that cracking initiates at the S45C near the interface and then propagates. This result indicates that the

bonding strength is higher than that of S45C after bonding. Considering these results, the control of constituent element diffusion is important for controlling the strength of specimens produced by SPF-DB.

Figure 4. The micrographs of crack propagation in the S45C-SPDSS interface for various number of cycles. Red line indicates the bonded interface. Lower part of red line is S45C [8].



However, the active diffusion of light elements in fine grain superplastic materials may be useful in surface hardening treatments, such as carburizing and boronizing processes.

3. Carburization and Boronization of Superplastic Duplex Stainless Steel

3.1. Solid Diffusion Carburization of SPDSS

The diffusion of carbon into SPDSS has been investigated using several methods. Three types of carburization apparatuses are shown in Figure 5. The carbon diffuses into surfaces exposed to carbon powder. Jauhari *et al.* performed carburization using the two kinds of apparatuses shown in Figures 5a and b [10]. For the apparatus shown in Figure 5a, a very small quasi-uniaxial pressure generated by thermal expansion is applied (hereafter, denoted by process A). For the apparatus shown in Figure 5b, a stress is applied to the compressed surface (hereafter, denoted by process B). For process B, Jauhari *et al.* was conducted at compressive stress of 74 MPa. Under this condition, some superplastic deformation would be expected at 1223 K; therefore to compare the result of process A and B, the difference of diffusion concurrent with superplastic deformation was observed. Recently, Ahamad *et al.* have investigated the diffusion concurrent with superplastic deformation using compression testing machine. The surface of the specimen exposed to the carbon, and then the sample compressed the strain rate of $1 \times 10^{-4} \text{ s}^{-1}$ up to the amount of compression strains 0.5 % at various temperatures [11]. Their experiment also demonstrates the relation between the superplastic deformation and diffusion. According to the above two papers, the presence of Fe-carbide and Cr-carbide on the surface was confirmed by X-ray diffraction. Further they estimated the activation energies (Q) from following procedure [10,11]. The carburized layer thickness (d) was defined as the texture difference obtained by scanning electron microscope (SEM) image. The carbon layer growth rate constant (K) was estimated by the annealing time (t) dependence of d using the equation as below:

$$d^2 = Kt \quad (1)$$

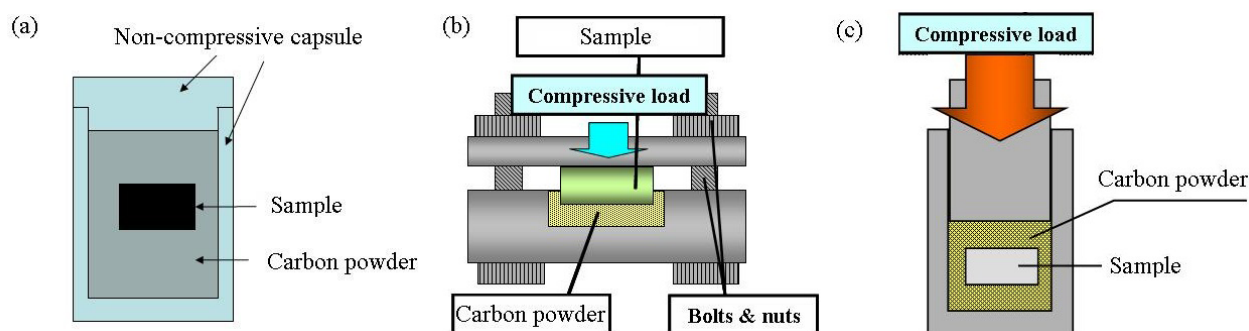
Q was estimated using following Arrhenius relation:

$$K = K_0 \exp(-Q/RT) \quad (2)$$

where K_0 , R and T are the constant, gas constant (8.314 J/mol K) and temperature, respectively.

According to the Q calculated in process A is 198.58 kJ/mol, whereas the Q of process B is 151.87 kJ/mol. Further, the Q obtained by Ahamad *et al.* was 174.08 kJ/mol [11]. Their process to obtained Q is the same as further experiments perform in same group;, therefore aforementioned value can be used for comparison. From their results, it can be considered that the uniaxial compressive stress decreases the energy barrier for the diffusion of carbon into SPDSS [10,11]. However the absolute value of Q obtained by the above mentioned method needs to be taken care of, due to the value of d obtained by SEM image. The d should be defined by concentration change; further it would be necessary to consider the reaction to the Fe and Cr in SPDSS.

Figure 5. Apparatuses used in previous carburization experiments.



Our group performed diffusion carburization experiments on both non-superplastic DSS and SPDSS using the apparatus shown in Figure 5c [12]. Carburization was performed using an evacuated compression testing machine at a compressive stress of 3 MPa.

Micrographs of the vertical cross-section of the compression face of both the non-superplastic DSS and SPDSS carburized at 1273 K for 30 min. are shown in Figure 6. To reveal the distribution of Cr-carbide, both cross-section surfaces were electrolytically etched using a 10% oxalic acid solution. The black region in the figure shows the etched area, namely, Cr-carbide area. It is clear that carbon diffuses into the SPDSS rather than the non-superplastic DSS. AES analysis results for the above mentioned SPDSS carburized method is shown in Figure 7a, which confirms C is near the compressed surface to carbon. From the line analysis result shown in Figure 7, the concentration of C shows drastic decrease to a depth of 50 μm inside the surface; a further small amount of C can be detected between the depths of 50 and 120 μm . The carburized layer thickness of 120 μm corresponds to that obtained in Figure 6a. Further, according to the line analysis result of Cr shown in Figure 7b, the concentration of Cr, is instable in carburized layer; however, in the non-carburized area the intensity of Cr is almost constant. It represents segregation of Cr caused by the diffusion of C.

Micrographs of the vertical cross-section of the compression faces of SPDSS, carburized at various temperatures in 30 min, are shown in Figure 8. The thickness of the carburized layer increases with increasing temperature.

Figure 6. Micrograph of the vertical cross-section of compression side faces of non-superplastic SPDSS (a) and non-superplastic DSS (b) carburized at 1273 K for 30 min [12]. The surfaces are electrolytically etched using a 10% oxalic acid solution.

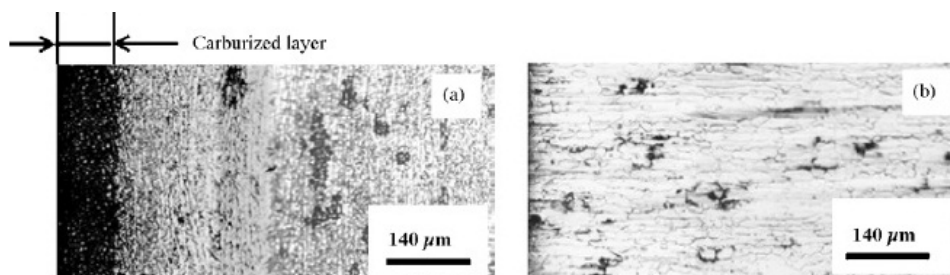


Figure 7. Concentration mapping for Carbon (a) and Chromium (b) obtained by auger electron spectroscopy of the vertical cross-section of compression side faces of SPDSS carburized at 1273 K for 30 min under 3 MPa. The bold yellow lines in figures are line analysis results for each element [12].

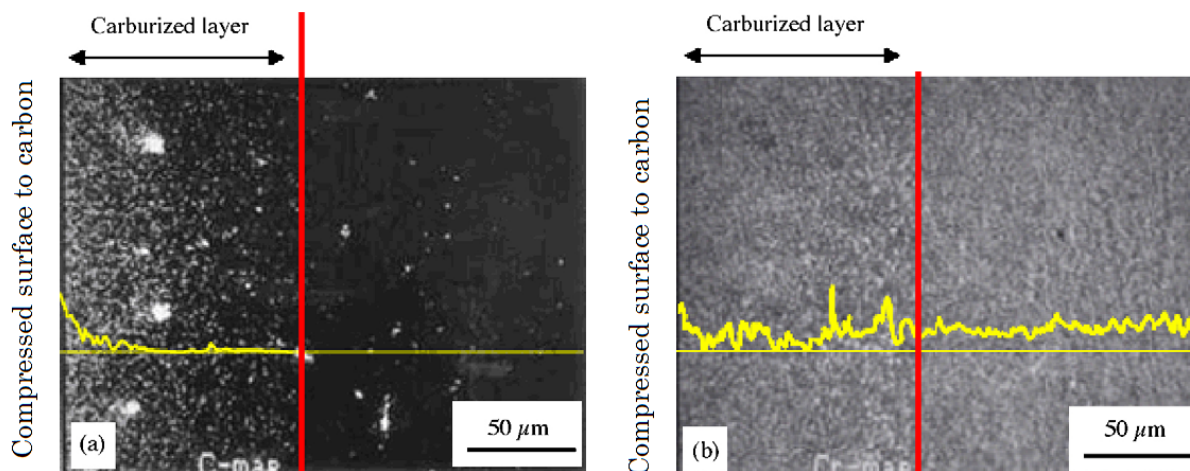
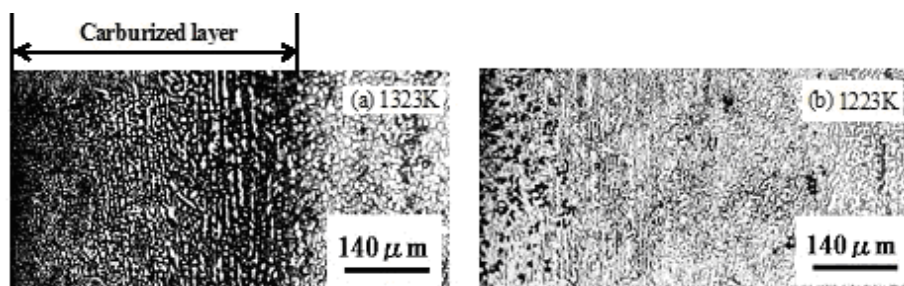
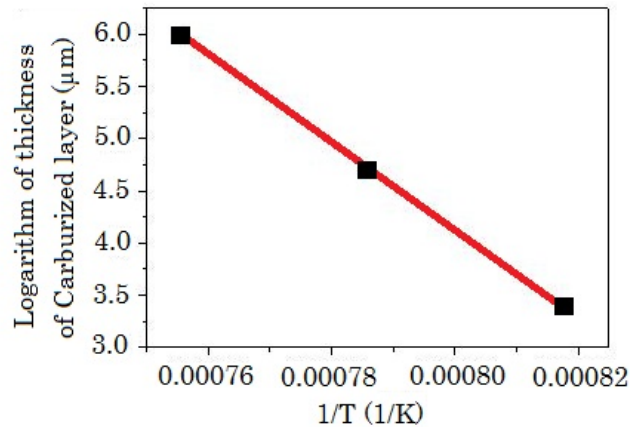


Figure 8. Micrograph of the vertical cross-section of compression faces of the SPDSS carburized at 1323 K (a) and 1223 K (b) for 30 min. The surfaces are electrolytically etched using a 10% oxalic acid solution.



An Arrhenius plot of the temperature dependence of the carburized layer thickness (t), defined by the micrograph of 10% oxalic acid solution electrolytically etched surface, is shown in Figure 9. The plot of $1/T$ is directly proportional to $\ln t$. This result indicates that the activation energy is the same in temperature range above 1223 K, namely, in the superplastic state.

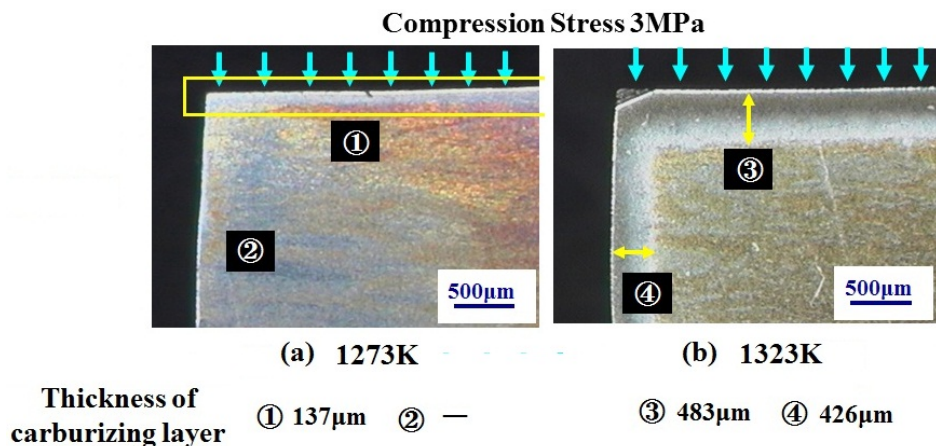
Figure 9. Arrhenius plot of the temperature dependence of the carburized layer thickness.



Micrographs of compression and non-compression faces carburized at 1273 and 1327 K are shown in Figure 10, respectively. At 1273 K shown in Figure 10a, the carburized layer is only confirmed on the compression face. However, at 1327 K, the carburized layer is clearly confirmed not only on the compression side but on the non-compression side as well. As results show that compressive stress activates the diffusion of carbon into the SPDSS, then the re-crystallization of microscopic grains is caused by heat activating the diffusion of carbon.

The Vickers hardness of a carburized layer is reported in references 10 and 11. The surface hardness of carburized layer made in process B under compression stress 74 MPa at 1223 K for 8h is higher than that of process A under very small stress [10]. On the other hand, according to the experiment of Ahamad *et al.* using compression testing machine at 1223 K for 84 min., the Vickers hardness of carburized layer is similar to the process A in reference 10. These results indicate two factors exist to increase Vickers hardness. One is the deformation, which is considered to promote the diffusion of carbon, and the other is time, which is considered to promote the reaction among carbon and comprising elements of SPDSS. The surface hardness mentioned in reference 10 reaches over 1000 Hv after carburization at a temperature of 1223 K for 8 h using process B. This value is comparable to that of hard type chemical Cr deposition coating.

Figure 10. Micrograph of compression and non-compression faces carburized at (a) 1273 and (b) 1327 K, respectively.



2.3. Solid Diffusion Boronization of SPDSS

The diffusion of boron into SPDSS has been investigated. Diffusion of boron has been investigated both in evacuated and atmosphere spaces, respectively. As a result, boron can diffuse into the SPDSS not only in an evacuated space but also in atmosphere. Further, our experiments cannot confirm that the variation depends on the compressive stress.

Auger electron spectroscopy (AES) maps of the distribution of boron in boronized non-superplastic DSS and SPDSS processed at 1273 K for 8 h are shown in Figure 11 [13]. A network-type distribution of boron is confirmed in the DSS as shown in Figure 11b, which indicates that boron diffuses along the grain boundaries. In the case of the SPDSS, boron shows inner grain diffusion. These results imply that the diffusion mode is different in SPDSS and non-superplastic DSS.

Figure 11. Auger electron spectroscopy maps of the distribution of boron in boronized non-superplastic SPDSS (a) and non-superplastic DSS (b) processed at 1273 K for 8 h [13].

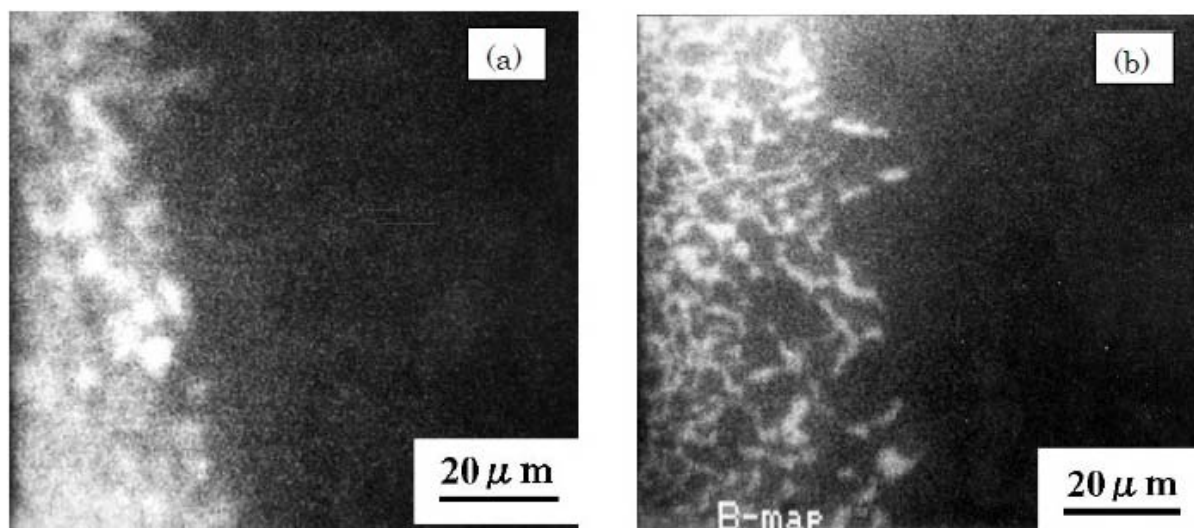
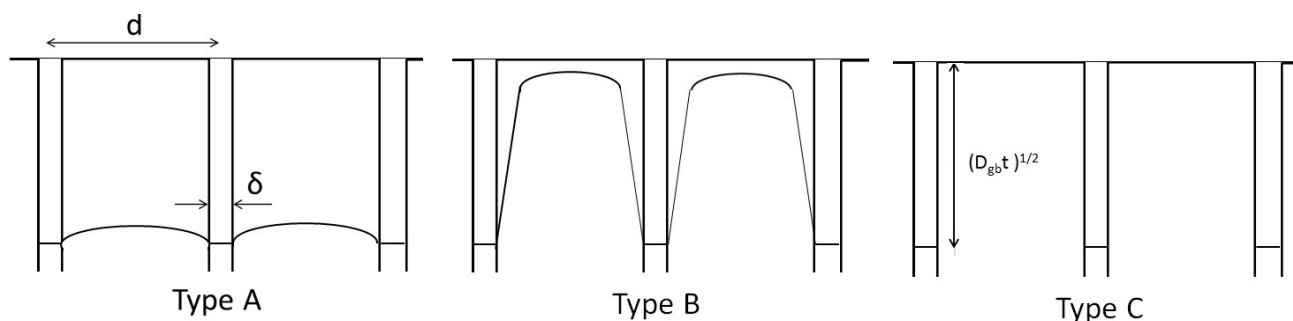


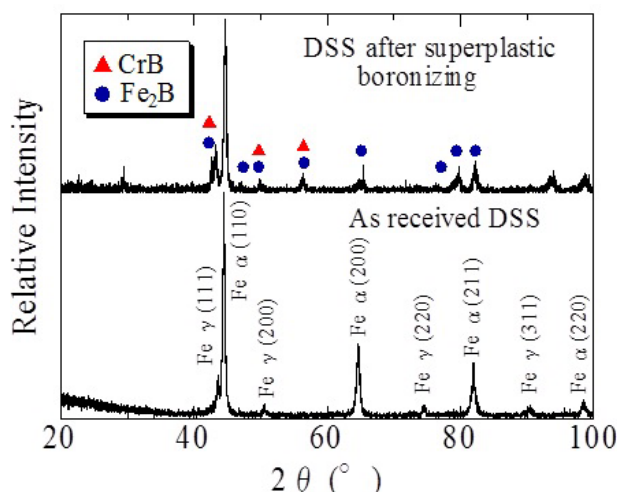
Figure 12. Classification of diffusion types according to Harrison. d and δ are grain width and grain boundary width, respectively. $(D_{gb}t)^{1/2}$ is grain diffusion length.



Diffusion was classified into three types by Harrison, as shown in Figure 12 [14]. In type C, diffusion occurs mainly along grain boundaries. Type A diffusion occurs under conditions of a long time or small grain sizes against the volume diffusion. Type B is the intermediate diffusion state between type A and C. Based on the boron distributions obtained by AES, the diffusion types of non-superplastic DSS and SPDSS are type C and type A, respectively. The grain size of the SPDSS is

clearly smaller than that of the non-superplastic DSS as shown in Figure 1. However, the fact that diffusion depends on stress in the superplastic state is taken into consideration; the variations in the grain boundary and dislocation densities must be discussed. Furthermore, if anomalous variation of the elastic constant, concurrent with lattice softening occurred, as predicted by theoretical studies [3], it was necessary to consider the variation of the volume diffusion coefficient.

Figure 13. X-ray diffraction pattern of boronized SPDSS [15].

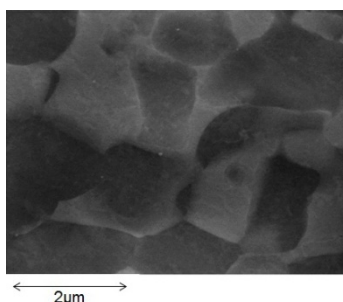


The XRD pattern of the boronized SPDSS is shown in Figure 13. This diffraction pattern indicates the generation of Cr boride and Fe boride [15,16]. From this result, very high hard surface will be expected.

4. Boronization of Duplex $\text{Ti}_{88.5}\text{Al}_{4.5}\text{V}_3\text{Fe}_2\text{Mo}_2$ Alloy

The diffusion of boron in duplex $\text{Ti}_{88.5}\text{Al}_{4.5}\text{V}_3\text{Fe}_2\text{Mo}_2$ alloy (hereafter called SP-700) provided by JFE Corporation has been investigated. SP-700 has very fine texture, as shown in Figure 13. This alloy shows superplasticity under strain rate of $2 \times 10^{-4} \text{ S}^{-1}$ above approximately 1023 K [17]. A surface of SP-700 was coated with boron powder, and a uniaxial compressive stress was applied in atmosphere and further annealed for 4 h at various temperatures.

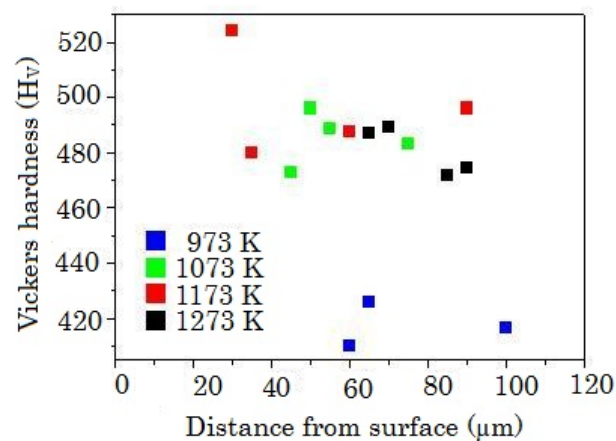
Figure 14. Scanning electron micrograph of SP-700.



Plots of the annealing temperature dependence of the Vickers hardness as a function of the distance from the surface coated with boron powder are shown in Figure 14. The Vickers hardness of the

annealing temperature above 1073 K is obviously higher than that of 973 K. Further, the diffusion of boron was confirmed by energy dispersive spectroscopy from the sample boronized at 1073 K. Considering these trends, the increase of Vickers hardness causes the diffusion of boron above superplastic transition temperature. The Vickers hardness decreases as the distance increases from the surface. The Vickers hardness values observed in the present experiments was lower than that of the borides of the element comprising SP-700, therefore borides were hardly formed.

Figure 15. Annealing temperature dependence of the Vickers hardness as a function of the distance from the surface coated with boron powder [18].



4. Conclusions

Experimental reports of the diffusion of carbon and boron in fine-grain superplastic alloys have been reviewed.

For superplastic duplex stainless steel, the diffusion of carbon and boron proceeds faster than in non-superplastic duplex stainless steel. Further, diffusion can be activated by uniaxial compressive stress.

The diffusion type differs for non-superplastic duplex stainless steel and superplastic duplex stainless steel. Non-superplastic duplex stainless steel shows typical grain boundary diffusion while inner grain diffusion was confirmed in superplastic stainless steel. Based on XRD results, Fe and Cr carbides or borides are formed, which means that the diffused carbon and boron react with the elements comprising the duplex stainless steel. The Vickers hardness of the carburized and boronized layers showed a higher value compared to that obtained with other surface treatments such as electro-deposition.

The diffusion of boron into the superplastic titanium-based alloy $Ti_{88.5}Al_{4.5}V_3Fe_2Mo_2$ was investigated. The hardness increased by annealing above the superplastic temperature. Below the superplastic temperature however, the hardness was not altered.

Acknowledgments

A part of Figures 2, 3 and 4 are reprinted materials of references 8 and a part of Figures 6 and 7 are reprinted materials of reference [11] with permission from Elsevier (license number 2644080042581, 2672610776162). Figure 11 is a reprinted material of ref 13 with permission from Springer (license number 2645640840695). Author deeply acknowledges the helpful discussion provided by Emeritus Professor

Hiroyuki Ogiyama of Ehime University. Further author also thanks for their useful discussion provided Tesuya Suko of Ehime University and Iswadi Jauhari of university of Malaya. Further Author also acknowledged technical help for experiments provided by Satoshi Okano, Hiromichi Aono, Toshiro Tanaka, Hiroaki Ohfuji, Shin-ichi Tanaka, Toshiki Hatano and Tetsuya Suko of Ehime University.

References

1. Nieh, T.G.; Wadsworth, J.; Sherby, O.D. *Superplasticity in Metals and Ceramics, Cambridge Solid State Science Series*; Clarke, D.R., Suresh, S., Ward, I.M., Eds.; Cambridge University Press: West Nyack, NY, USA, 2007.
2. Saito, T.; Furuta, T.; Hwang, J.-H.; Kuramoto, S.; Nishino, K.; Suzuki, N.; Chen, R.; Yamada, A.; Ito, K.; Seno, Y.; *et al.* Multi-functional alloys obtained via a dislocation-free plastic deformation mechanism. *Science* **2003**, *300*, 464-467.
3. Soucatis, P.; Katsnelson, M.I.; Simak, S.; Ahuja, R.; Eriksson, O.; Mohn, P. First principle calculation of superplastic transition-metal alloys. *Phys. Rev. B* **2004**, *70*, 012201:1-012201:3.
4. Lagos, M. Theory of superplasticity in polycrystalline material: Stress-induced structural instability of grain boundaries. *Phys. Rev. B* **2005**, *71*, 224117:1-224117:15.
5. Hiraga, T.; Miyazaki, T.; Tasaka, M.; Yoshida, H. Mantle superplasticity and its self-made demise. *Nature* **2010**, *468*, 1091-1094.
6. Hefti, L.D. Innovations in the superplastic forming and diffusion bonded process. *J. Mater. Eng. Perform.* **2008**, *17*, 179-182.
7. Xun, Y.W.; Tan, M.J. Applications of superplastic forming diffusion bonding to hollow engine blades. *J. Mater. Proc. Technol.* **2000**, *99*, 80-85.
8. Matsushita, M.; Ogiyama, H.; Suko, T.; Matsuda, S. Study on solid state welding of duplex stainless steel with carbon steel based on superplasticity and consideration of the cyclic fatigue fracture behavior. *Mater. Chem. Phys.* **2009**, *114*, 522-524.
9. Jauhari, I.; Ogiyama, H.; Tsukuda, H. Solid state diffusion bonding of superplastic duplex stainless steel with carbon steel. *Mater. Sci. Res. Int.* **2003**, *9*, 154-159.
10. Jauhari, I.; Rozali, S.; Masdek, N.R.N.; Ogiyama, H. Surface properties and activation energy analysis for superplastic carburizing of duplex stainless steel. *Mater. Sci. Eng. A* **2007**, *466*, 230-234.
11. Ahamad, N.W.; Jauhari, I.; Azis, S.A.A.; Aziz, N.H.A. Surface properties and activation energy of superplastically carburized duplex stainless steel. *Mater. Chem. Phys.* **2010**, *112*, 454-458.
12. Matsushita, M.; Suko, T.; Matsuda, S.; Ohfuji, H.; Ogiyama, H. Analysis of the texture of superplastic carburized duplex stainless alloy. *Mater. Chem. Phys.* **2009**, *114*, 522-524.
13. Matsushita, M.; Ogiyama, H. Diffusion of Boron on superplastic duplex stainless steel. *J. Phase Equilib. Diffus.* **2010**, *31*, 2-5.
14. Harrison, L.G. Influence of dislocations on diffusion kinetics in solids with particular reference to alkali halides. *Trans. Faraday Soc.* **1961**, *57*, 1191-1199.
15. Suko, T. Diffusion coating using superplastic phenomenon of ($\alpha + \gamma$) Duplex Stainless Steel. Master Thesis. Department of Mechanical Engineering, Ehime University: Matsuyama, Japan, 2008.

16. Jauhari, I.; Yusof, H.A.M.; Rozali, S.; Ogiyama, H. Effect of powder particle size on the development of ultra hard surface through superplastic boronizing of duplex stainless steel. *J. Solid Mech. Mater. Eng.* **2007**, *1*, 1-8.
17. Ishikawa, M.; Kuboyama, O.; Niikura, M.; Ouchi, C. *Titanium'92: Science and Technology*; 1st ed.; Froes, F.H., Ed.; TMS: Warrendale, PA, USA, 1993; p. 141.
18. Tanaka, S.; Hatano, T. Boronization of Superplastic duplex $\text{Ti}_{88.5}\text{Al}_{4.5}\text{V}_3\text{Fe}_2\text{Mo}_2$ alloy. Graduation Thesis. Department of Mechanical Engineering, Ehime University: Matsuyama, Japan, 2011.

© 2011 by the authors; licensee MDPI, Basel, Switzerland. This article is an open access article distributed under the terms and conditions of the Creative Commons Attribution license (<http://creativecommons.org/licenses/by/3.0/>).